16 Topical Seminar on Innovative Particle and Radiation Detectors (IPRD23)
Siena, 25 - 29 September 2023

Characterization of Teledyne e2v LGADs

EG Villani

IPRD23 Siena, Sep. 2023

Outline

- Introduction: LGADs for timing
- Te2v LGAD design and simulations
- Test results
- Summary & conclusions

Introduction: Timing for HL-HLC

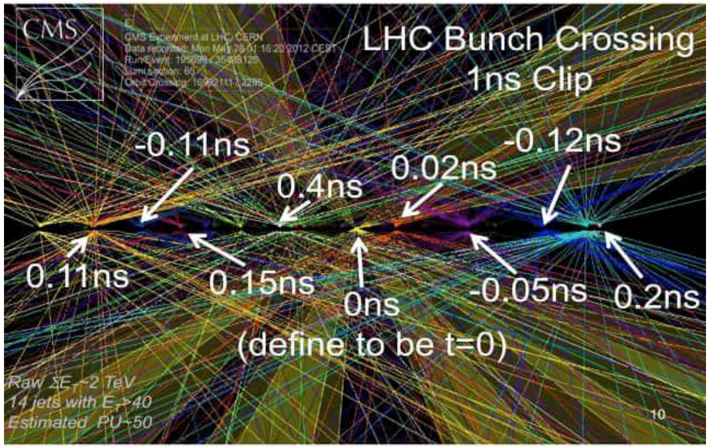

Interaction time of many pp vertexes happening in the same bunch crossing at LHC in the case of ≈50 overlapping events. The vertexes are spaced 10’s of ps apart

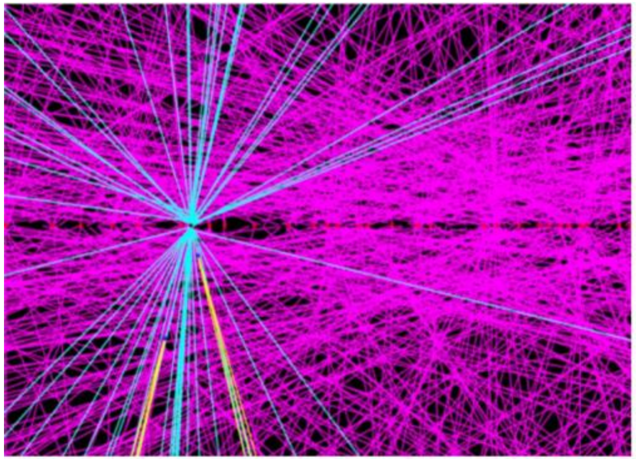

ATLAS simulation of spatial events at HL-LHC with < μ >= 140 pileup

At the nominal luminosity of the LHC the average number of pp interactions in a single bunch crossing (pileup) is approximately 23

The planned luminosity upgrade to HL-LHC will increase this number to about 200

The increased spatial pileup line density (number of collisions / unit length along the beam axis) will lead to misidentified tracks

Introduction: Timing for HL-HLC

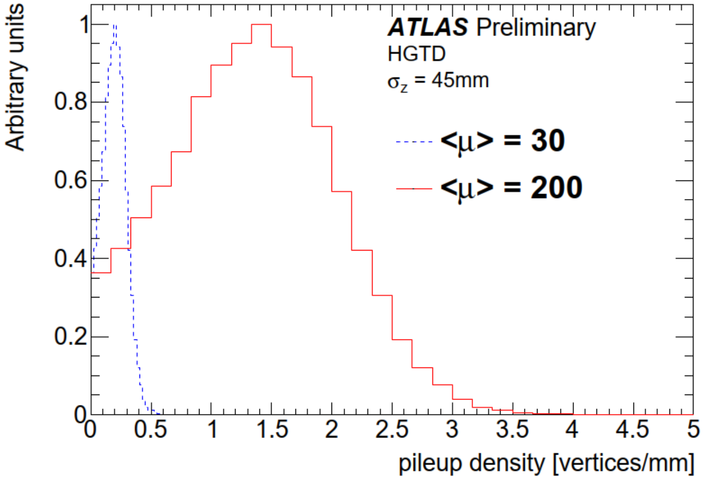

Simulation of HL-LHC local pileup vertex densities for two values of < μ >= 30 and < μ >= 200 ≃ 1.44 vertices/mm MPV

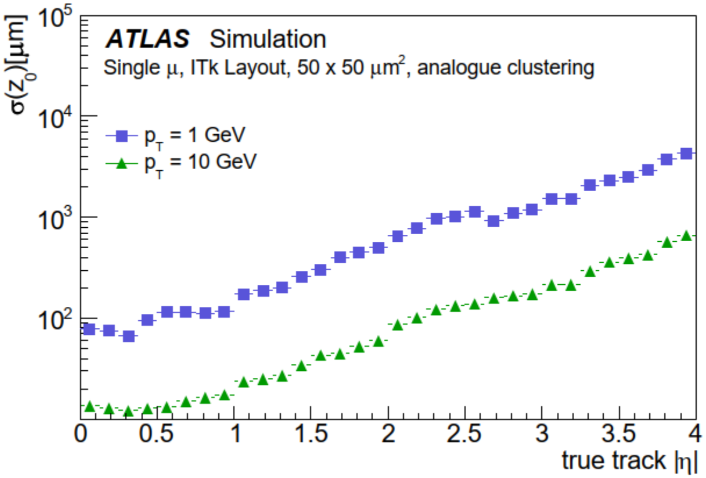

Resolution of the longitudinal track impact parameter, z0, as a function of η for muons of pT = 1 GeV and pT = 10 GeV using ITk alone

Track reconstruction becomes particularly critical at high η, when resolution becomes larger than distance between vertices

One solution to suppress the detrimental effect of pileup on reconstruction is to separate vertices in time beside in space. A timing resolution of ≃ 30 ps would provide an almost complete pileup suppression

In ATLAS the High Granularity Timing Detector (HGTD) for pileup suppression and luminosity measurement has been proposed to complement the Inner Tracker (Itk) in the forward region

Introduction: Timing for HL-HLC

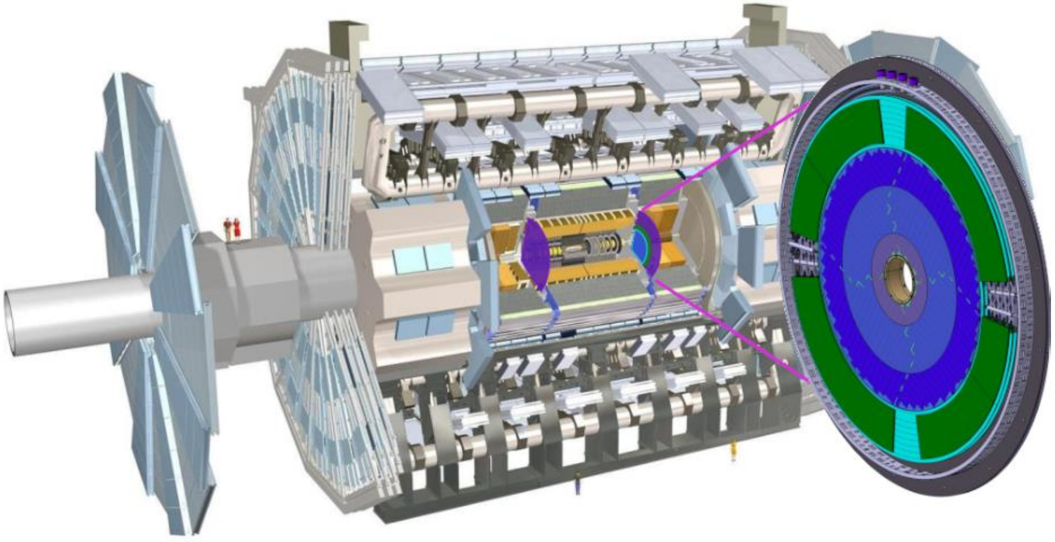

Position of the HGTD within the ATLAS Detector. Positioned at $z = \mp 3.5$ m along the beamline, on both sides of the detector

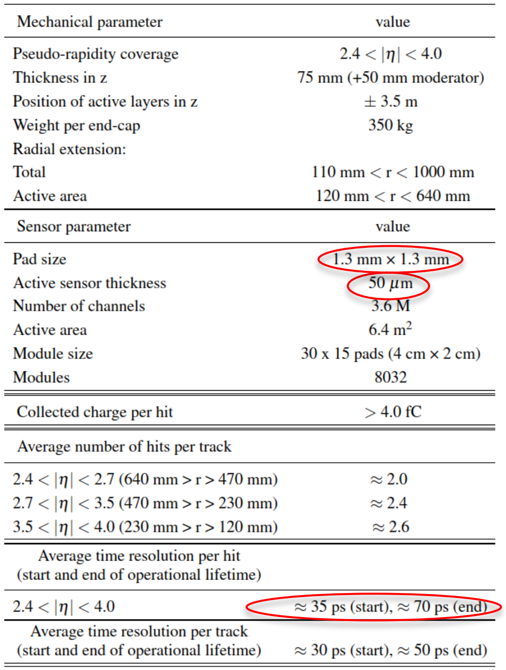

Mechanical parameter	value
Pseudo-rapidity coverage	$2.4 < \|\eta\| < 4.0$
Thickness in z	75 mm (+50 mm moderator)
Position of active layers in z	$\pm$ 3.5 m
Weight per end-cap	350 kg
Radial extension:	
Total	110 mm < r < 1000 mm
Active area	120 mm < r < 640 mm
Sensor parameter	**value**
Pad size	1.3 mm × 1.3 mm
Active sensor thickness	50 μm
Number of channels	3.6 M
Active area	6.4 m^2
Module size	30 x 15 pads (4 cm × 2 cm)
Modules	8032
Collected charge per hit	> 4.0 fC
Average number of hits per track	
$2.4 < \|\eta\| < 2.7$ (640 mm > r > 470 mm)	≈ 2.0
$2.7 < \|\eta\| < 3.5$ (470 mm > r > 230 mm)	≈ 2.4
$3.5 < \|\eta\| < 4.0$ (230 mm > r > 120 mm)	≈ 2.6
Average time resolution per hit (start and end of operational lifetime)	
$2.4 < \|\eta\| < 4.0$	$\approx$ 35 ps (start), $\approx$ 70 ps (end)
Average time resolution per track (start and end of operational lifetime)	$\approx$ 30 ps (start), $\approx$ 50 ps (end)

The HGTD in ATLAS will be placed in the gap region between the barrel and the end-cap calorimeter. Two instrumented double-sided layers on two cooling/support disks on each end-cap.

Timing sensors used in HGTD are based on Low Gain Avalanche Detector (LGAD) technology

[1] ATLAS Collaboration, Technical Design Report: A High-Granularity Timing Detector 2562 for the ATLAS Phase-II Upgrade, tech. rep. CERN-LHCC-2020-007, CERN, 2020, URL: 2563 https://cds.cern.ch/ record/2719855.

LGAD for timing

PIN

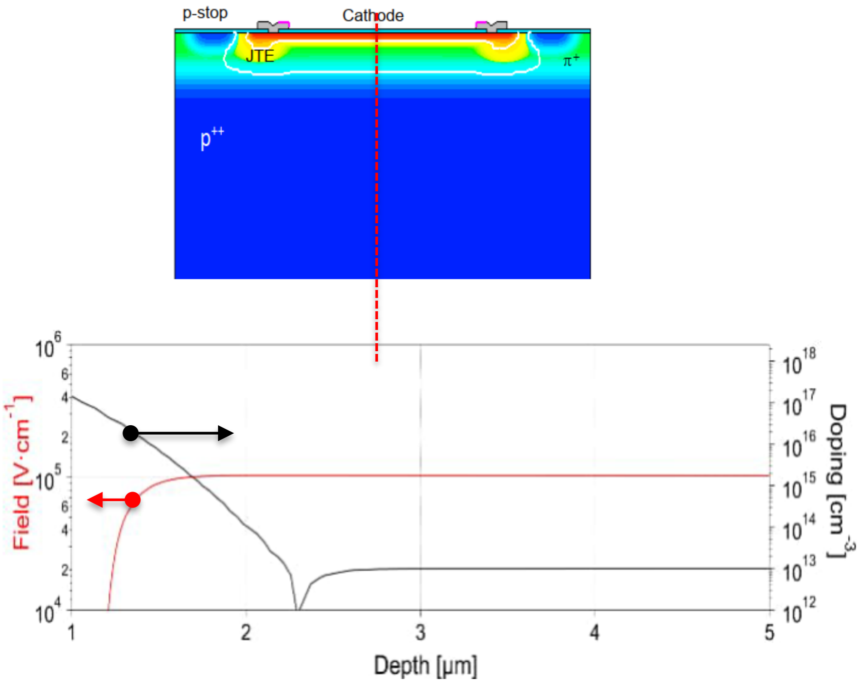

LGAD

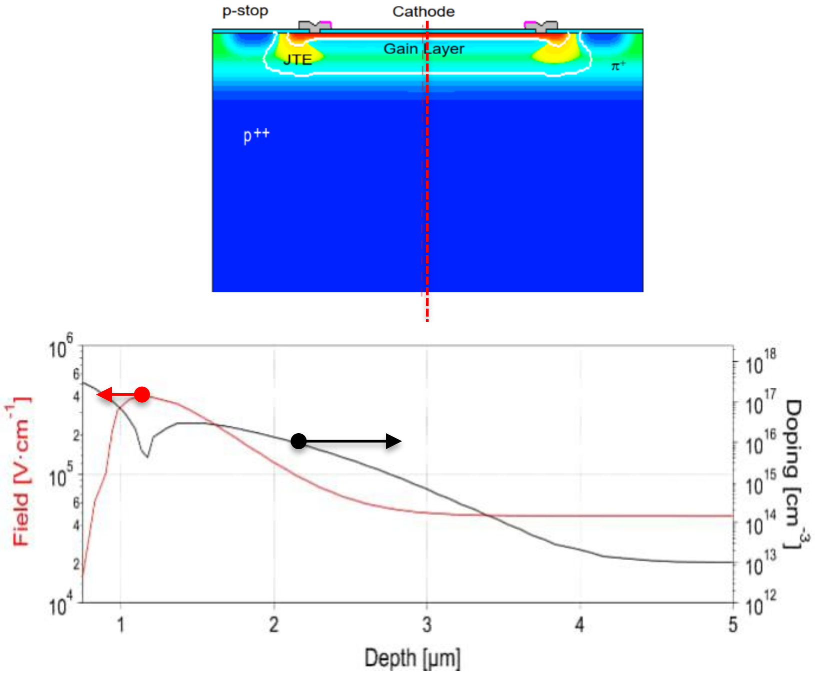

A standard PIN silicon sensor consists essentially of a pn junction. At depletion it shows an ~ uniform electric field F

In the LGAD device an additional p^+ doped layer (gain layer or GL) is implanted near the pn junction. When depleted the GL creates an electric field high enough ($\simeq 3\cdot10^5\ \mathrm{V/cm}$) to start impact ionization, leading to charge multiplication by a factor G

LGAD for timing

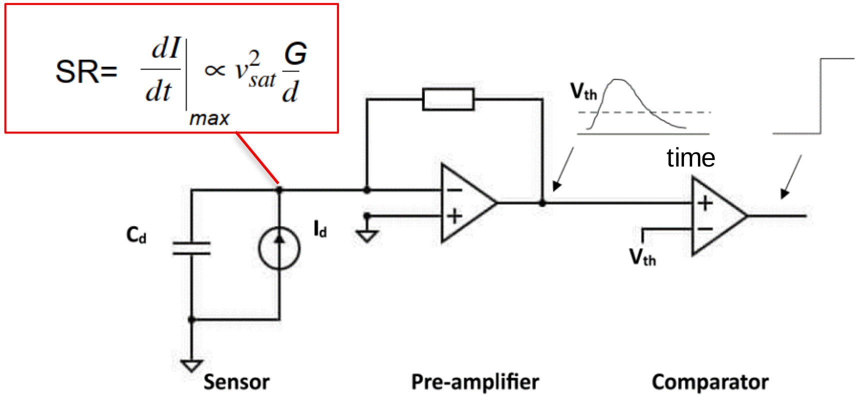

$$SR=\left.\frac{dI}{dt}\right|_{max} \propto v_{sat}^2\frac{G}{d}$$

$$\sigma_t^2=\sigma_{ioniz}^2+\sigma_{dist}^2+\sigma_{jit}^2+\sigma_{TDC}^2$$

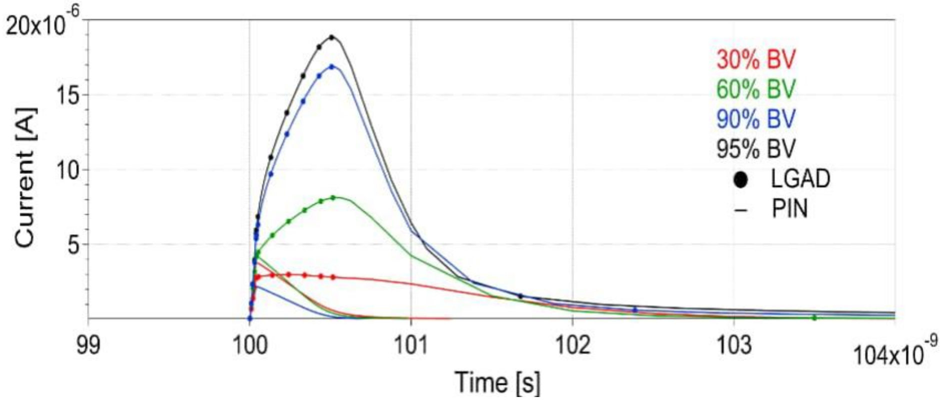

TCAD simulation of LGAD / PIN signal vs. V_{bias}

In a sensor with an internal charge gain G the peak signal amplitude I_{max} and the slew rate $\frac{dI}{dt_{max}}$ increase, leading to high time resolution

Increasing the gain increases the noise faster, reducing the S/N

Teledyne e2v LGAD design

LGAD PIN

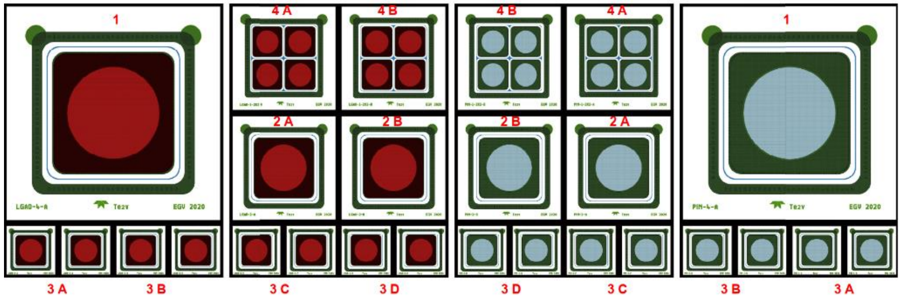

Cell layout	Cathode diameter	Laser hole diameter	Cathode to p-stop	p-stop width	p-stop to Guard Ring	Guard Ring width
1	4000	3020	156	6	152	332
2	2000	1510	78	6	76/96	166
3	1000	755	39	6	38/48/58/68	83
4	1000	755	39	6	38/68	166

Size of Run I cells [um]

Two runs of LGAD fabrication with Teledyne 2ev (Te2v) on 6 inch HR 50 um epi wafer :

Run I included 1,2, 4 and 2x2 of 1x1 mm^2 cells

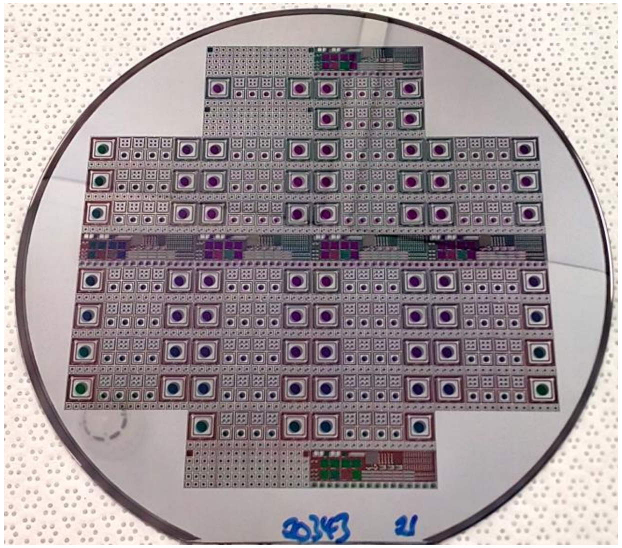

Wafer	GL dose	GL energy
19,20,21	1.00	1.00
17,18	1.07	1.00
15,16	0.92	1.05
12,13,14	1.00	1.05
9,10,11	1.07	1.05
7,8	1.15	1.05
4,5,6	1.00	1.11
2,3,24	1.07	1.11

Normalized values of GL 11B doping

Teledyne e2v LGAD design

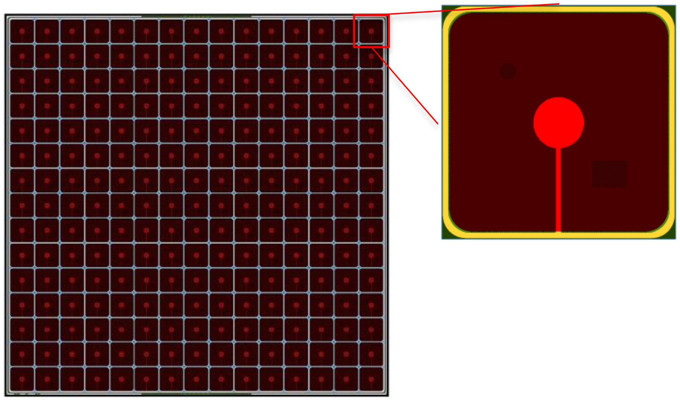

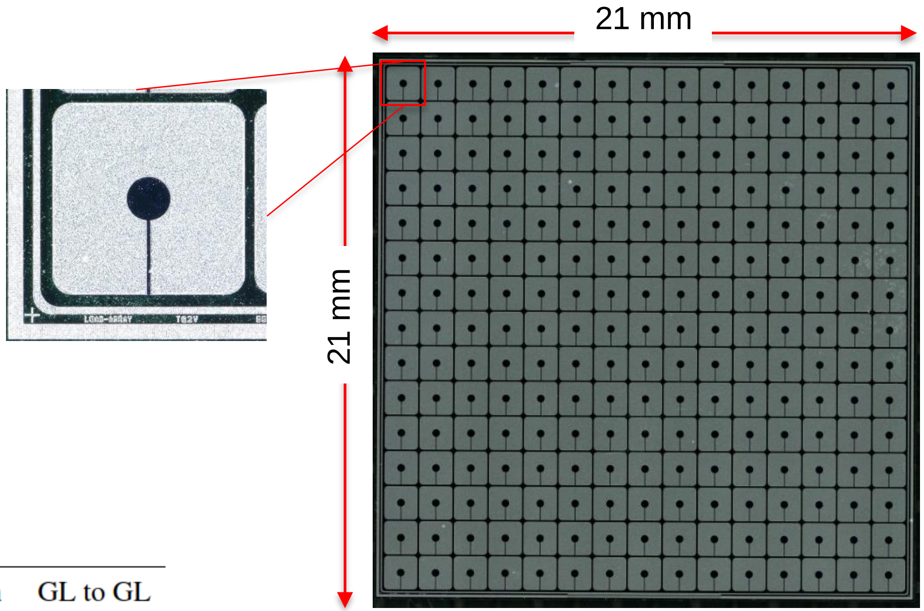

Cathode diam.	Cath to GR	Cath to p-stop	p-stop width	Cath to Cath	GL to GL
1300	83	30	6	66	86

Size of Run II cells [um]

Second fabrication (Run II) included array of 15 x 15 cells of 1.3 x 1.3 mm^2

Wafer	GL dose	GL energy
1	1.00	1.00
2	0.95	1.07
3	1.00	1.07
4	1.00	0.93

Normalized values of GL 11B doping

Teledyne e2v LGAD TCAD simulation fabrication process

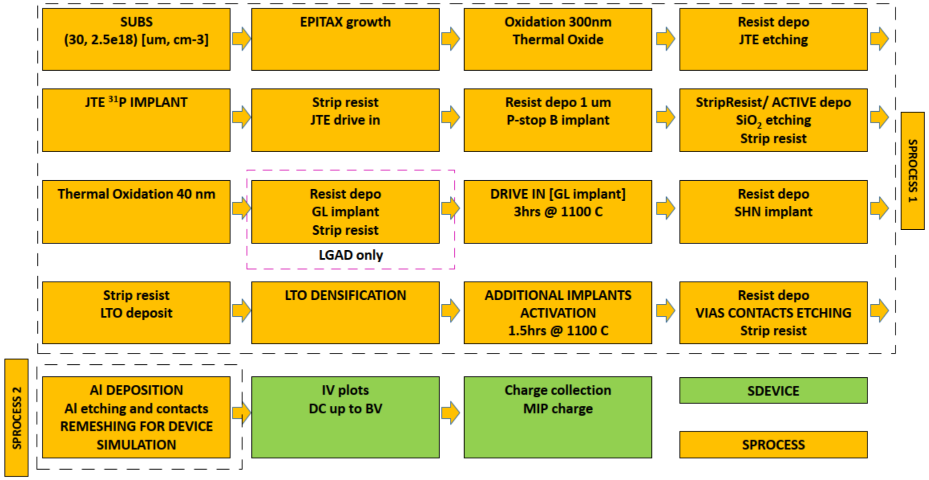

SUBS (30, 2.5e18) [um, cm-3]

EPITAX growth

Oxidation 300nm Thermal Oxide

Resist depo JTE etching

JTE ^{31}P IMPLANT

Strip resist JTE drive in

Resist depo 1 um P-stop B implant

StripResist/ ACTIVE depo SiO$_2$ etching Strip resist

Thermal Oxidation 40 nm

Resist depo GL implant Strip resist

LGAD only

DRIVE IN [GL implant] 3hrs @ 1100 C

Resist depo SHN implant

Strip resist LTO deposit

LTO DENSIFICATION

ADDITIONAL IMPLANTS ACTIVATION 1.5hrs @ 1100 C

Resist depo VIAS CONTACTS ETCHING Strip resist

SPROCESS 1

SPROCESS 2

Al DEPOSITION Al etching and contacts REMESHING FOR DEVICE SIMULATION

IV plots DC up to BV

Charge collection MIP charge

SDEVICE

SPROCESS

Fabrication process flow

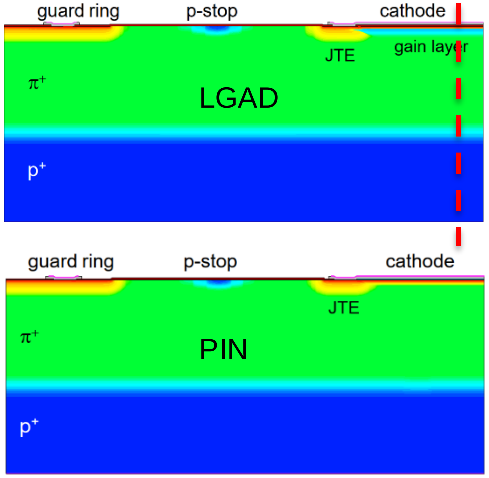

TCAD PIN and LGAD structure

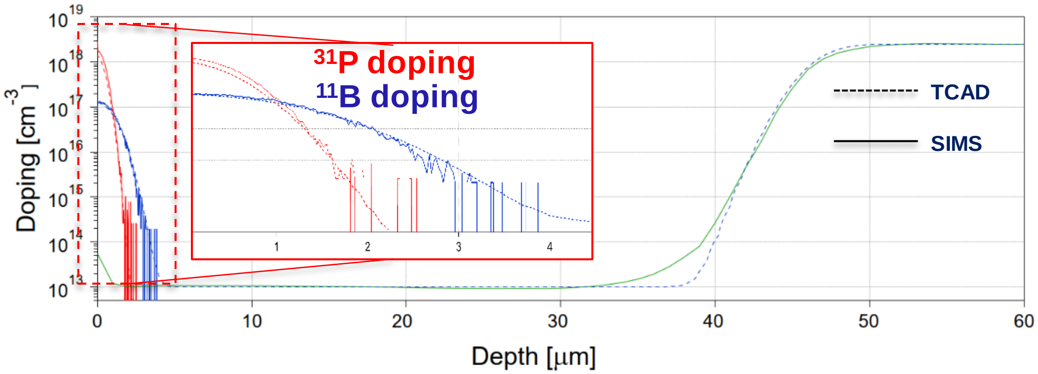

Wafer 2	Nominal	SIMS	TCAD	error
^{11}B dose [cm^{-2}]	1.45x10^{13}	1.51x10^{13}	1.44x10^{13}	-4%
^{11}B absolute peak [cm^{-3}]	NA	1.35x10^{17}	1.24x10^{17}	-8%
^{11}B GL peak [cm^{-3}]	NA	3.79x10^{16}	3.41x10^{17}	-10%
^{11}B GL peak depth [μm]	NA	1.394	1.519	+9%

TCAD and SIMS WF2 doping comparison

Full process simulation using Synopsys TCAD to predict doping profiles compared with SIMS measurements. Both MC (for ^{11}B) and analytical profiles (^{31}P) were used

Teledyne e2v LGAD TCAD simulation DC characteristics

$$L_D = \sqrt{\frac{\varepsilon_S k_B T}{e^2 N}}$$

The mesh size was set smaller than the **Debye length** L_D which sets the length scale of charge redistribution at interface between two regions of different doping. Around < 1 nm minimum mesh size used here

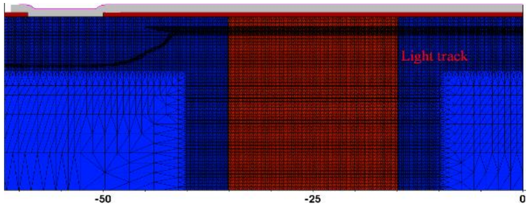

$$t_{dr} = \frac{\varepsilon_S}{eN\mu}$$

The time step during dynamic simulations was set smaller than the **dielectric relaxation time** t_{DR} which sets the typical time for the majority carriers fluctuations to decay under the field they produce. Around 1 ps for IR injection down to 50 fs for MIP

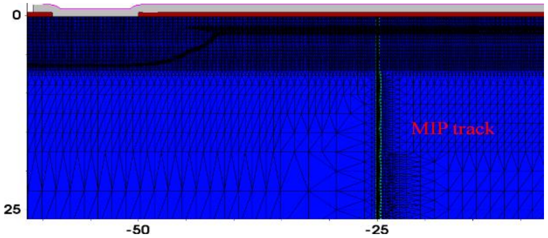

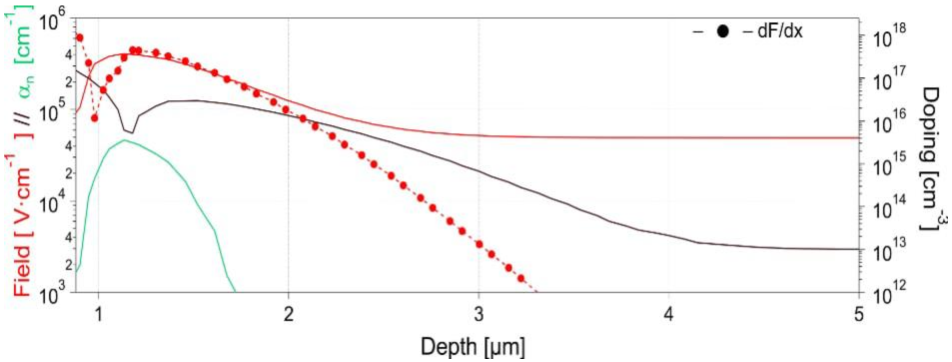

Electric field F, dF/dx , Doping and α_n *of LGAD biased at 90% BV along middle of GL*

Impact ionization is a non-local process. The related ionization coefficient (the probability per unit distance that a carrier impact ionizes along the direction of the field) usually depends not only on the local value of the field but also on the previous history of the carrier. Under the conditions:

$$\frac{1}{\alpha(F_m)}\frac{1}{F_m}\frac{dF}{dx} < 1$$

a local model can be assumed to be valid (the only possible default modelling in TCAD)

Teledyne e2v LGAD TCAD simulation
DC characteristics

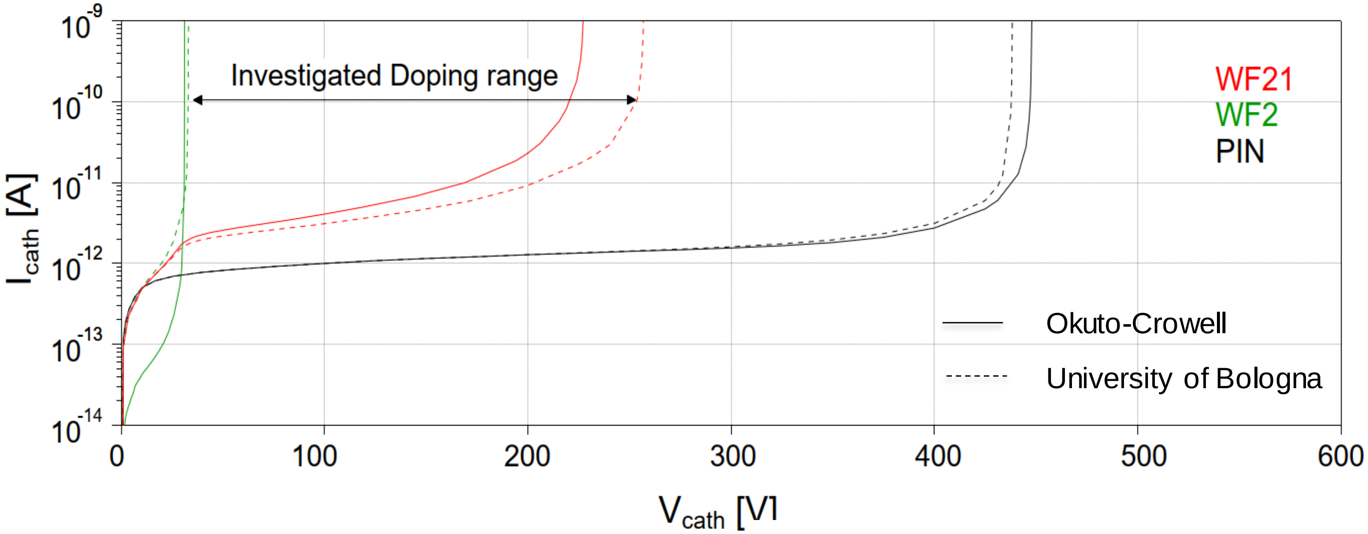

$$\alpha_\nu(F_{ava}) = \frac{F_{ava}}{a(T) + b(T)e^{\frac{d(T)}{F_{ava}+c(T)}}}$$

University of Bologna (δ=1)

$$\alpha_\nu(F_{ava}) = a(1+c(T-T_0))F_{ava}^{\gamma}e^{-\left(\frac{b(1+d(T-T_0))}{F_{ava}}\right)^{\delta}}$$

Okuto-Crowell (δ=2)

TCAD estimated Breakdown voltage of LGAD of different gain layer doping.
Two ‘extremes’ impact ionization models were used, as they represent limits of Shockley (δ=1) and Wolff (δ=2) theory. Other models (Baraff) are not by default available in TCAD.
The two extremes of Vbd correspond to doping configuration of the LGAD gain layer that were then chosen as bounding limits for the ^{11}B implant and related thermal processes.

Teledyne e2v LGAD TCAD simulation
Charge collection and gain

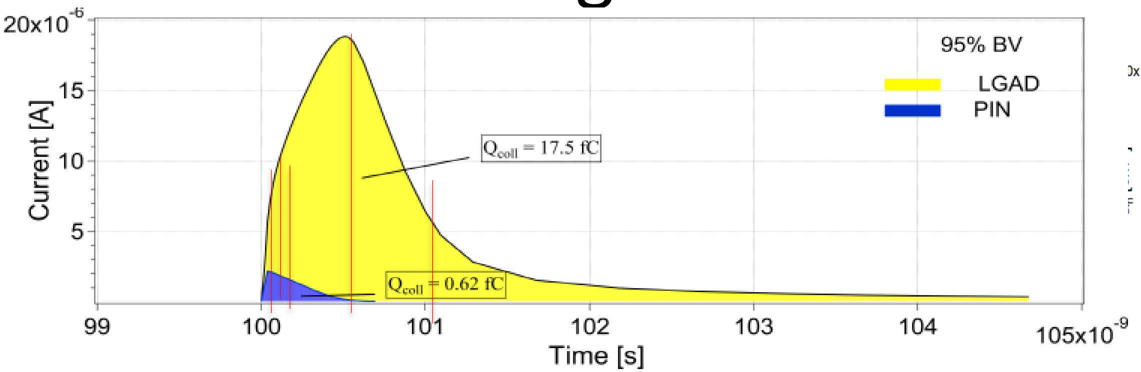

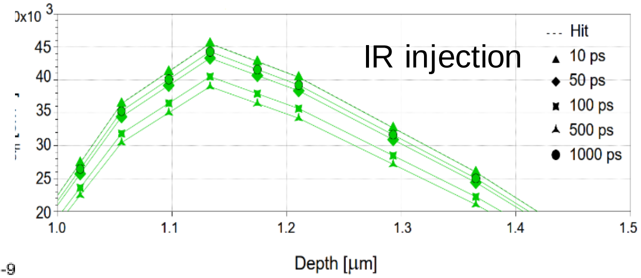

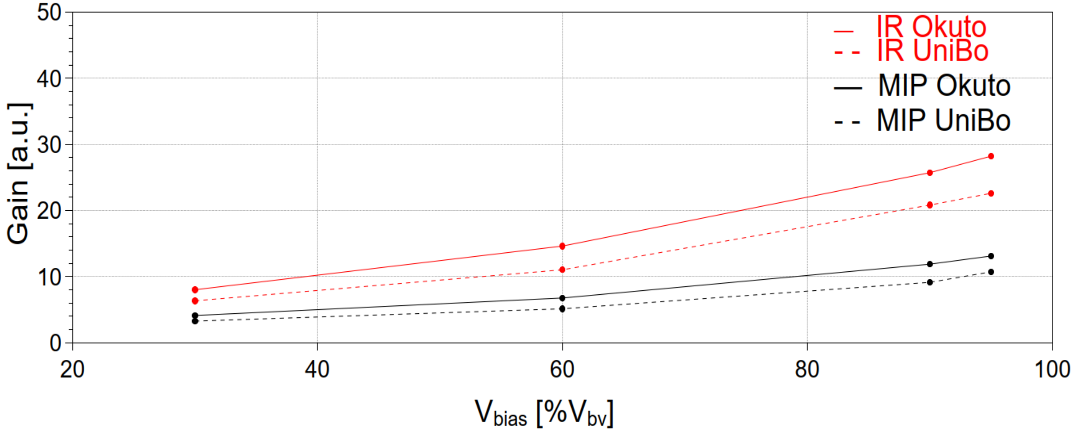

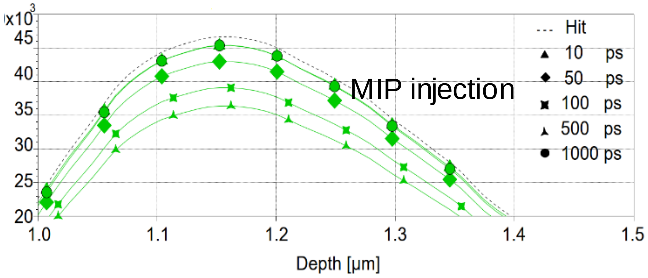

Transient simulation to estimate charge collection and gain performed both using Laser (1064 nm) and MIP injection

Gain obtained from ratio of collected charge by LGAD vs. bias compared to charge collected by PIN diode under same biasing conditions

Prediction of Gain suppression

Teledyne e2v LGAD Test setup

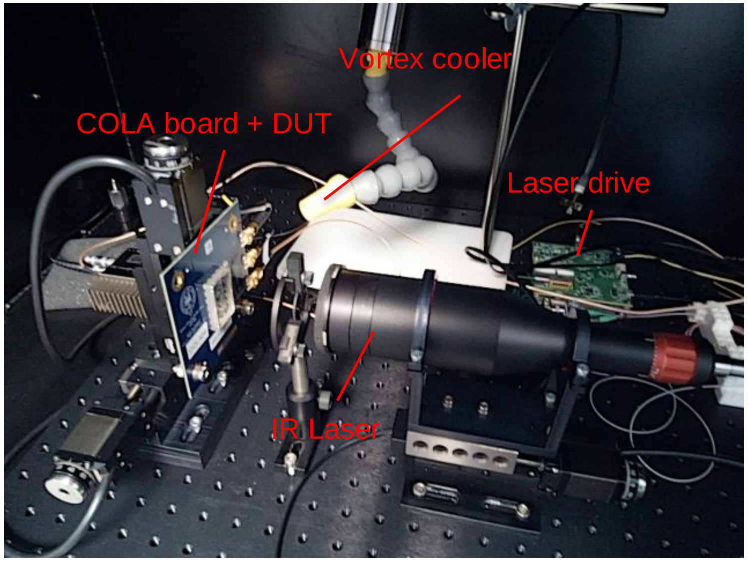

OPMD Oxford Laser setup

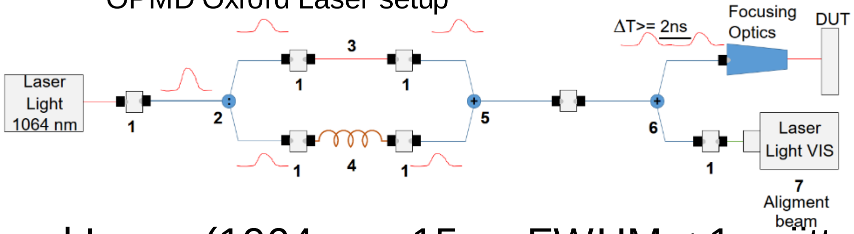

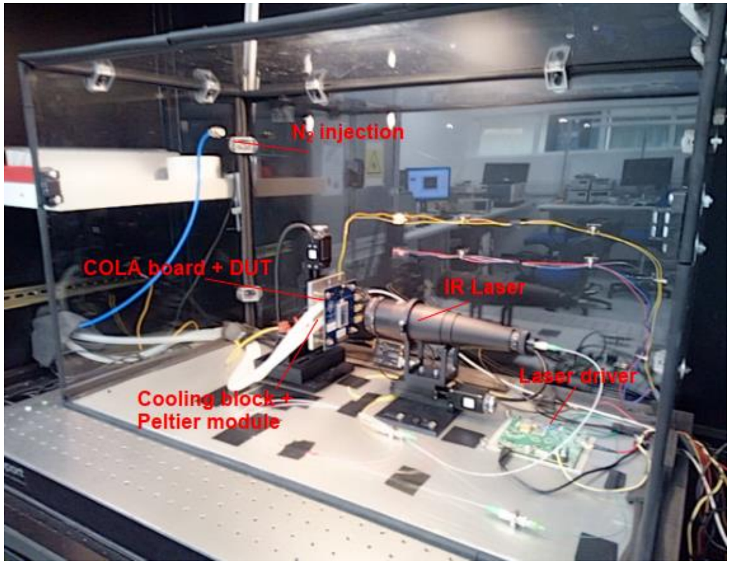

RAL Laser setup

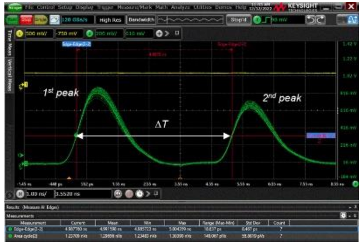

Infrared Laser (1064 nm -15 ps FWHM < 1ps jitter) charge injection

Laser calibrated to deliver < 1fC in PIN

Gain measured as ratio of collected charges LGAD/PIN

Jitter measured using Split Recombine method at different Constant Fraction Discriminator (CFD) value

Teledyne e2v LGAD Test setup

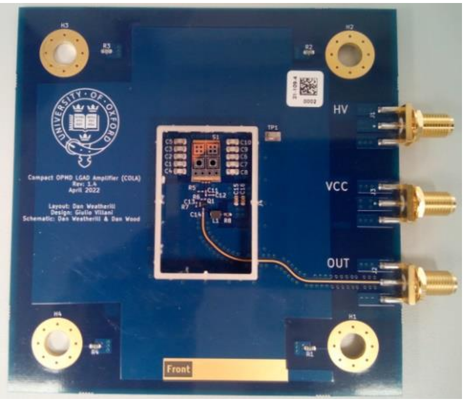

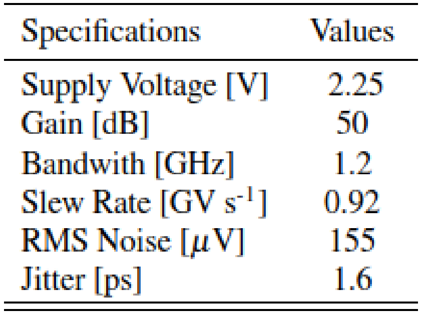

Specifications	Values
Supply Voltage [V]	2.25
Gain [dB]	50
Bandwith [GHz]	1.2
Slew Rate [GV s^{-1}]	0.92
RMS Noise [μV]	155
Jitter [ps]	1.6

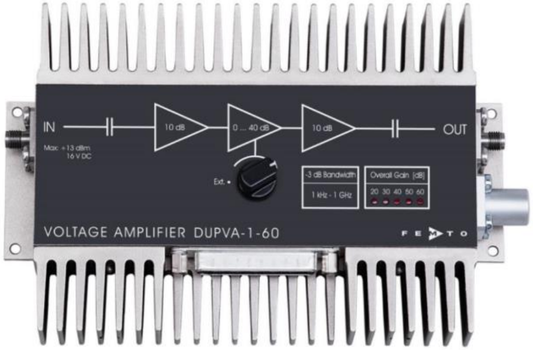

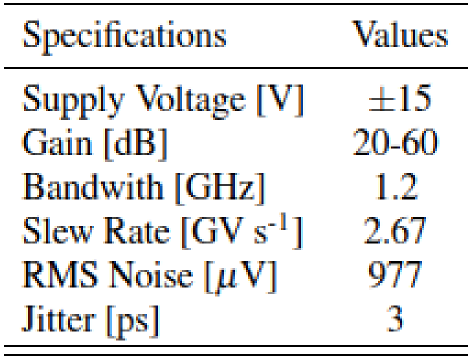

Specifications	Values
Supply Voltage [V]	±15
Gain [dB]	20-60
Bandwith [GHz]	1.2
Slew Rate [GV s^{-1}]	2.67
RMS Noise [μV]	977
Jitter [ps]	3

The LGAD output is amplified using two stages:

COLA (Compact OPMD LGAD Amplifier) designed at Oxford Physics Microstructure Detector (OPMD), 50 dB gain

Variable gain amplifier (set to 30 dB)

Jitters were measured using a Tabor Lucid 12 GHz LS1292B signal generator

The scope used was a Keysight Infinium model UXR0134A 128 Gsa/sec ~ 2.25 ps TDC error

Teledyne e2v LGAD Test setup

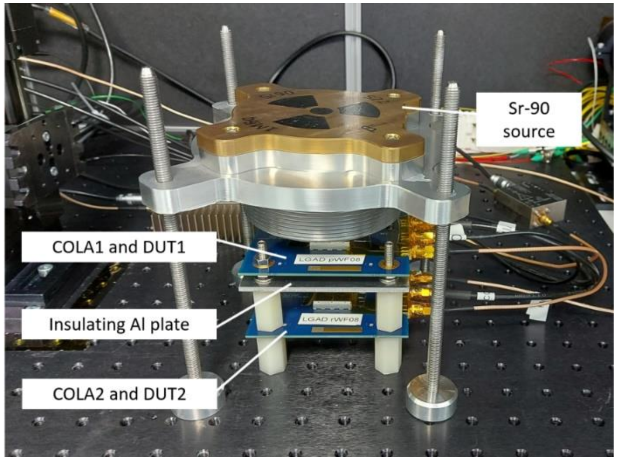

OPMD Source test setup

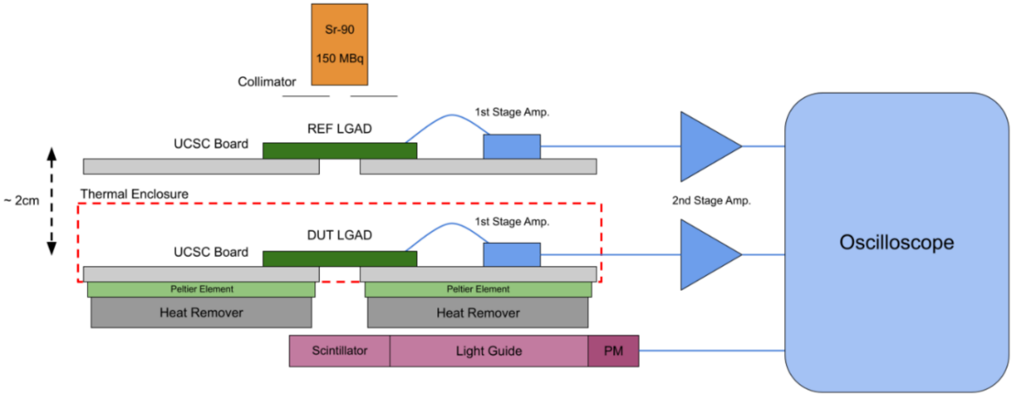

Birmingham Source test setup

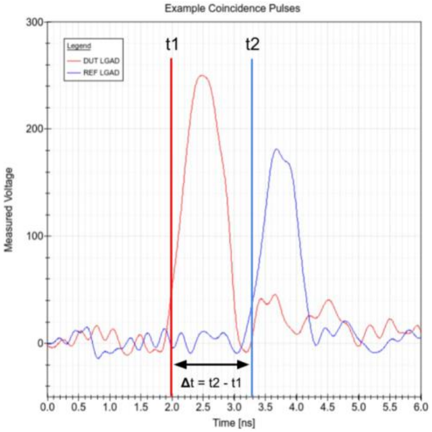

Example of a signal response from two LGADs detecting the same electron

Test using 90Sr source (Oxford OPMD – Birmingham)

Time resolution by taking sigma of fitted Gaussian to delay distribution

Teledyne e2v LGAD Test results - IV

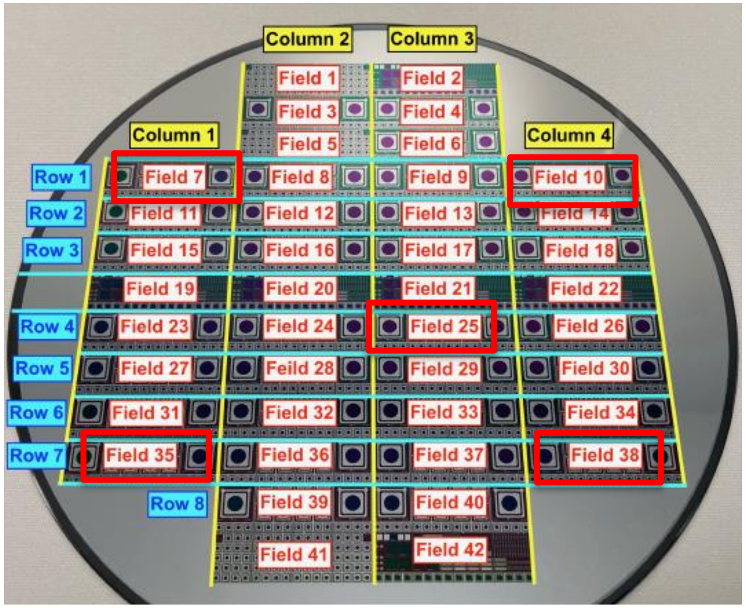

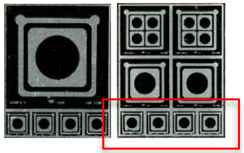

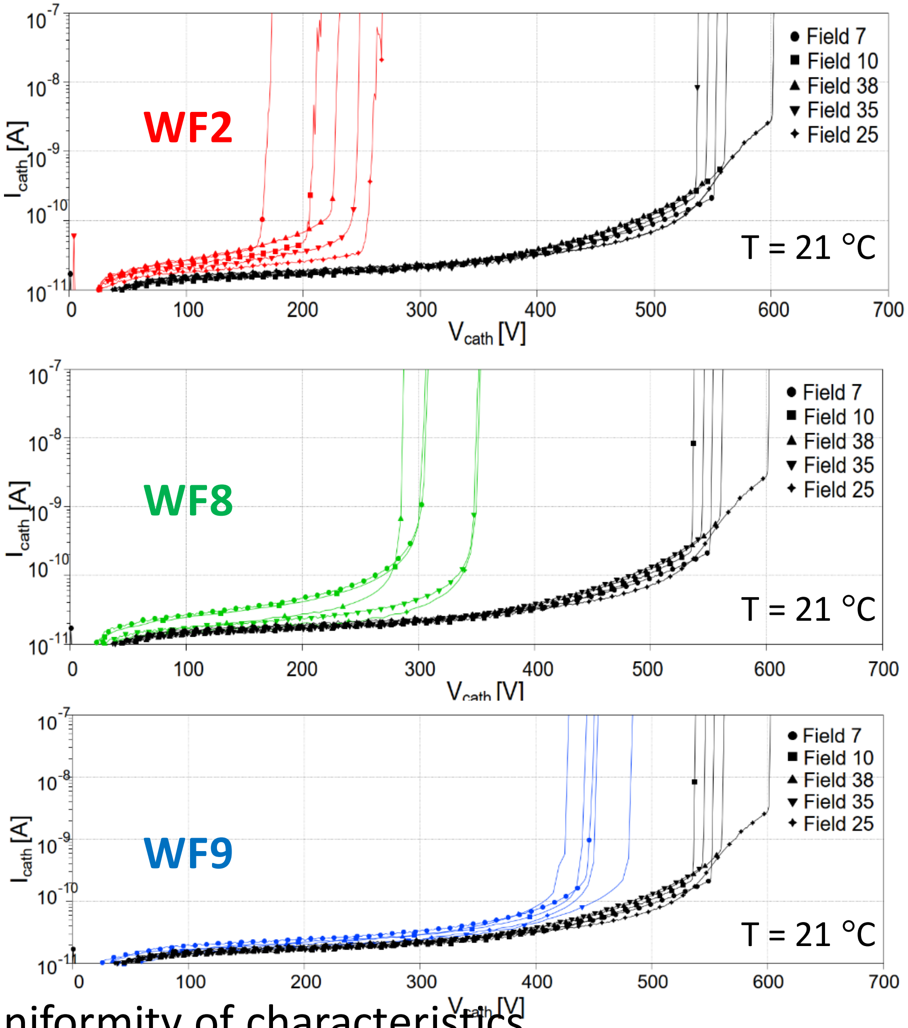

IV plots of 1 mm LGAD WF2, WF8 and WF9

Different areas on the wafer to investigate uniformity of characteristics

Typical LGAD leakage @ 90% BV around 10nA/cm2 @ RT

Teledyne e2v LGAD test results – Charge collection and Gain

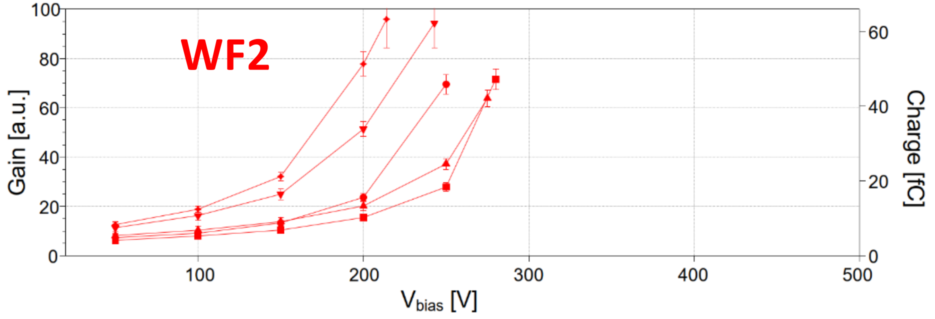

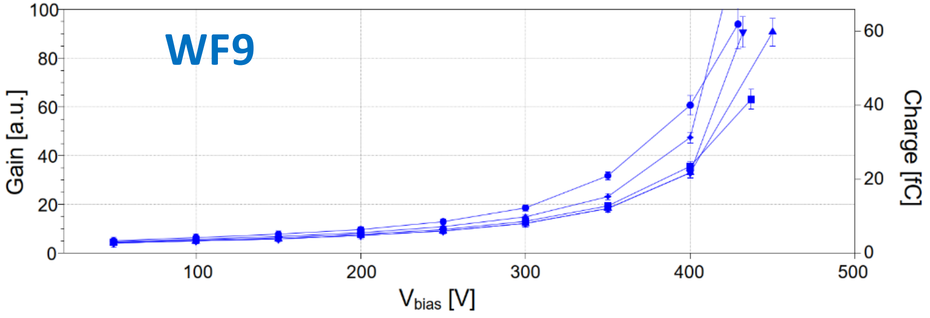

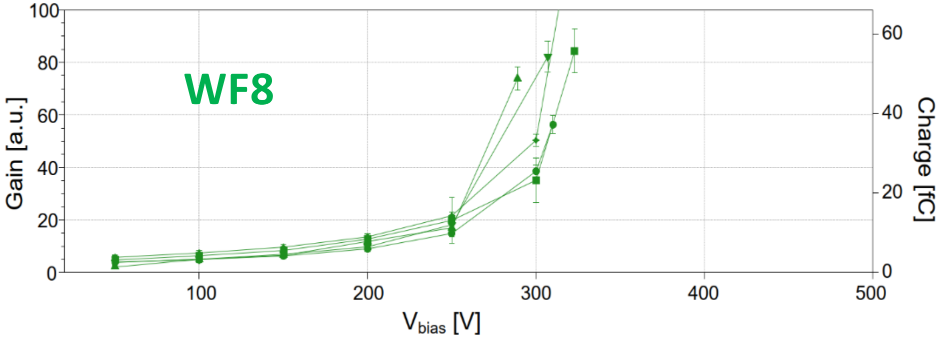

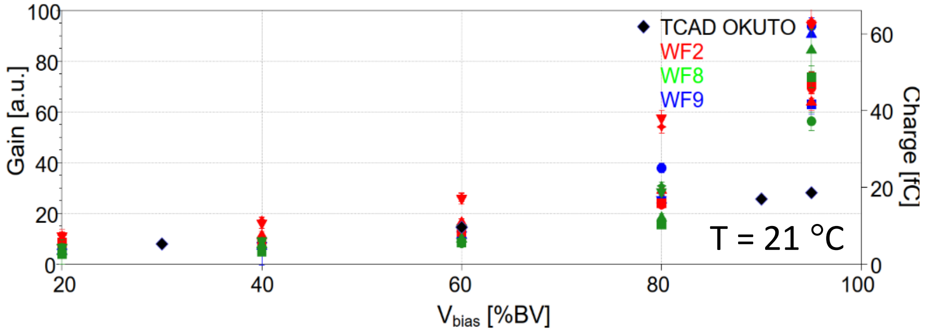

Gain plots using laser injection ~ 0.7 fC

Plot of gain vs. V_{bias}/V_{bv} shows similar trend for all flavours tested up to ~ 80 %V_{bv}

CFD value	V_{bv} 20%	V_{bv} 40%	V_{bv} 60%	V_{bv} 80%	V_{bv} 95%
25%	173.2 ± 34.1	45.56 ± 6.02	22.06 ± 3.7	11.56 ± 1.95	9.72 ± 0.8
50%	157 ± 9.34	47.36 ± 6.35	22.82 ± 4.08	11.88 ± 2.36	10.46 ± 0.99
90%	172.4 ± 22.07	66.98 ± 7.86	53.6 ± 6.61	50.36 ± 4.89	49.82 ± 2.76

TCAD comparison shows good prediction up to ~ 80 %V_{bv}

Teledyne e2v LGAD test results – timing results

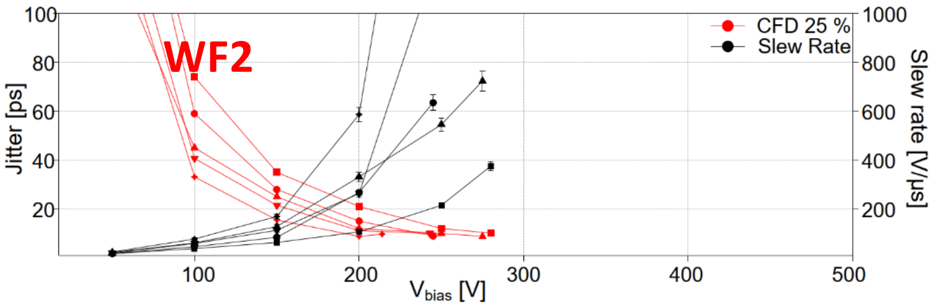

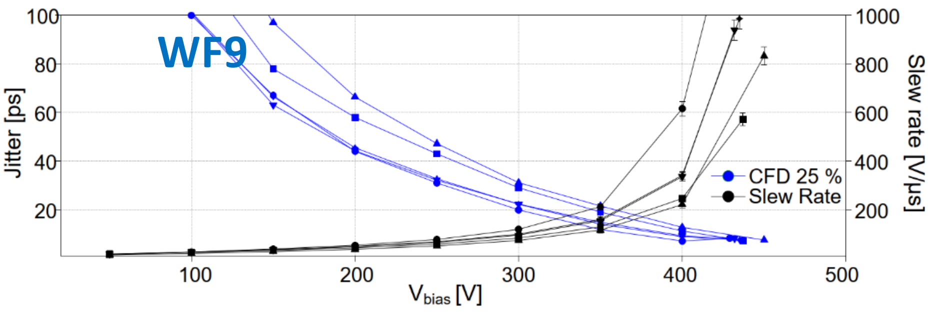

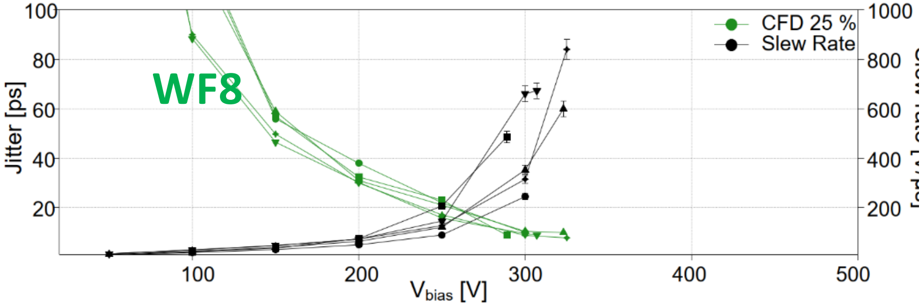

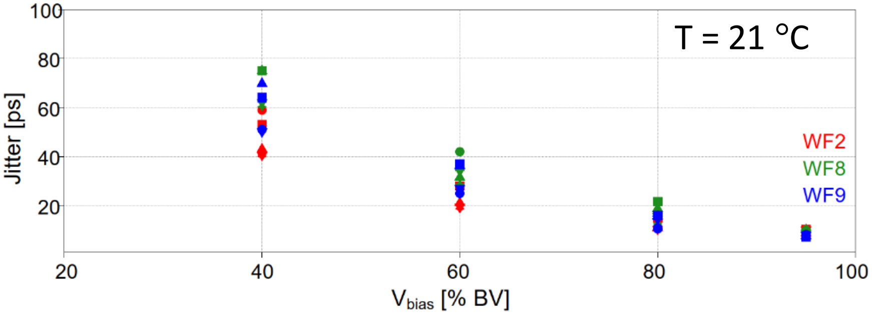

Jitter plots using laser injection ~ 0.7 fC

Plot of jitter vs. V_{bias}/V_{bv} shows similar trend for all flavours tested, converging to a common value

Minimum jitter ~ 10 ps @ 90-95% of BV using CFD = 25 %

Teledyne e2v LGAD test results – timing results

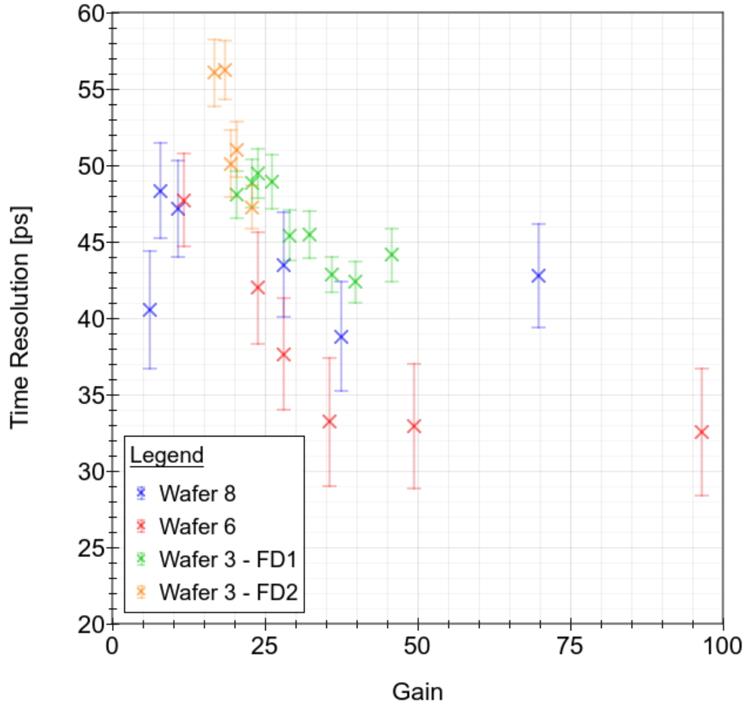

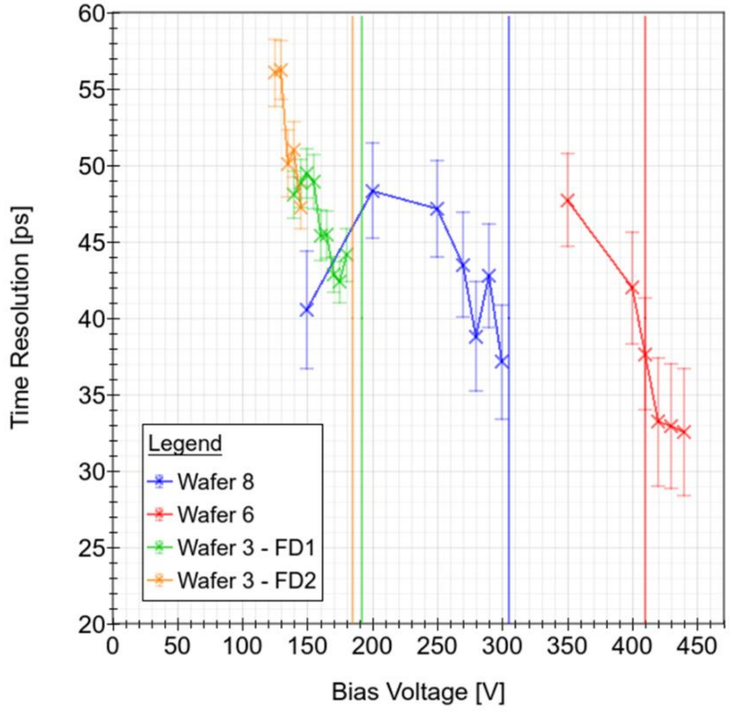

Timing plot using ^{90}Sr setup at University of Birmingham

For non-irradiated sensors time resolution of approximately 33 ∓ 4 ps

Teledyne e2v LGAD test results – timing results

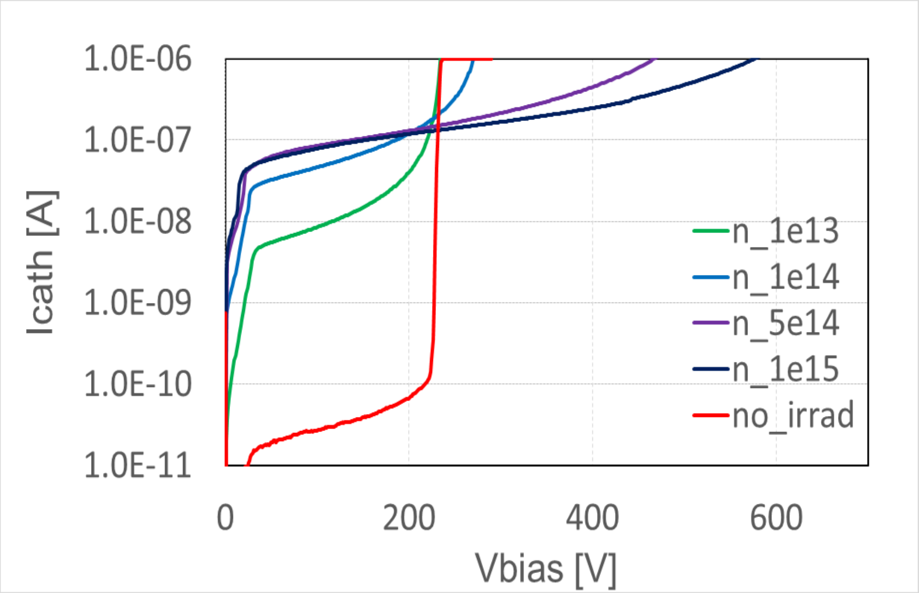

IV plot of WF2 n-irradiated LGAD

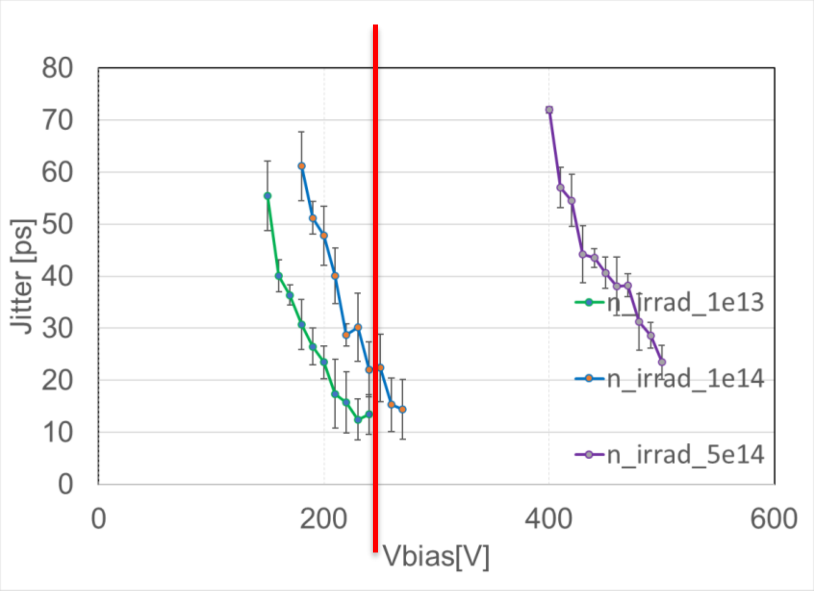

Jitter plot of #3 WF2 n-irradiated LGAD

Neutron irradiation campaign – LGAD were irradiated al Ljubljana (reactor n) up to fluence of 1e16 cm^{-2} and at Birmingham (26 MeV p) up to 5e14 cm^{-2}

Devices were annealed at 60 °C for 80 mins before tests

Testing ongoing

UKRI Science and Technology Facilities Council

Particle Physics

Teledyne e2v LGAD – low LET dosimetry

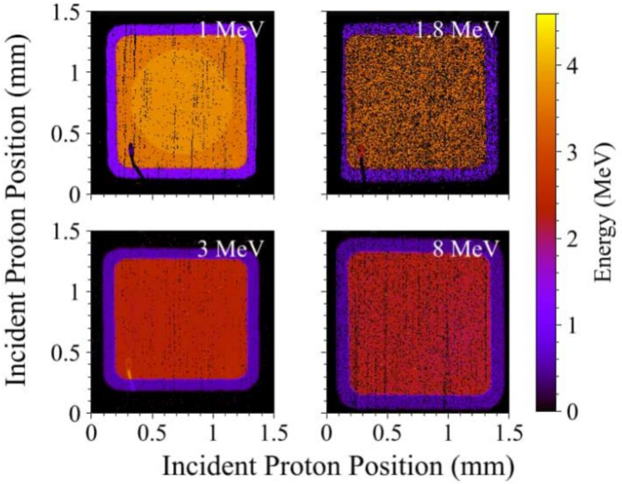

Median energy deposition maps for protons of varying energy incident on the Type 4 LGAD from WF2.Bias voltage 180 V

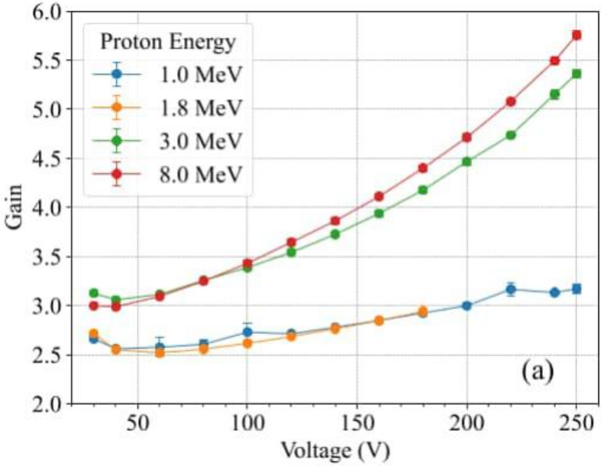

Resulting gain for protons of different energy incident on the Type 4 LGAD from WF2

Space radiation environment consists of a considerable amount of solar particle events (SPE), essentially low bursts of low LET particle. Also the reduction of out-of-field doses, of low-LET particles, is one of the challenges to improve long-term survival of patients following radiotherapy.

The intrinsic gain of LGAD devices is a possible solution to improve the signal to noise ratio for low LET dosimetry application*

*'A Two-Dimensional Characterisation of Low Gain Avalanche Diodes for Low-LET Microdosimetry',J. Archer, E.G. Villani et al,,presented at ANSTO User Meeting - AUM2023 – paper submitted to IEEE TNS

Summary and conclusions

- The increased pileup at HL-LHC represents a challenge for track reconstruction.

Using Ultra Fast detectors with time resolution of around 30 ps would help disentangle the tracks. The High Granularity Timing Detector (HGTD) in ATLAS has been designed for this purpose. It uses Low Gain Avalanche Detector (LGAD) as timing sensors

- This projects described the two runs of LGAD fabrication with Teledyne e2v. First run of individual cells designed to investigate achievable performances using the technology, the second a full LGAD array to HGTD specs

- TCAD simulations have been used in all phases of sensor design, including fabrication and charge collection. Gain prediction match test results up to 80 % of BV

- Test results indicate time resolution for non-irradiated sensors of around 34 ps using MIP and around 10 ps jitter using IR Laser light. Neutron Irradiated sensors show jitter of around 25 ps up to 1e14 fluence (ongoing tests)

- Initial tests done to investigate possible uses of LGAD for Low Let particles detection.

THANK YOU